DOI: 10.30511/pcdp.2025.2074998.1052 - ISSN: 3060-8376 - Vol 3(1), 2026

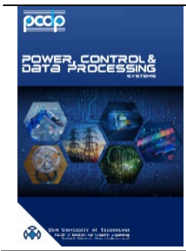

POWER, CONTROL AND DATA PROCESSING SYSTEMS

Available Online at: https://pcdp.qut.ac.ir/

Integrated Energy Management with P2G and CAES for Price Arbitrage and Renewable Utilization in Smart Grids

ARTICLE INFO

Article Type
Original Research

Authors
Mahdieh Monemi Bidgoli [1,*]
Milad Asadi [2]

[1] Independent Researcher, Kashan, Iran, m.monemi.b@gmail.com
[2] Independent Researcher, Shiraz, Iran, milad.asadi14@gmail.com

**** Correspondence***
Address: Independent Researcher, Kashan, Iran.
Phone: -
Fax: -
m.monemi.b@gmail.com

Article History
Received: October 17, 2025
Accepted: December 25, 2025
ePublished: March 01, 2026

ABSTRACT

Electric vehicles and hydrogen and gas storage systems, provide significant flexibility for energy management in the smart grid. This paper extends the integrated management framework of renewable energy resources, demand response programs, and water systems by incorporating two advanced electricity storage technologies: Power-to-Gas (P2G) and Compressed Air Energy Storage (CAES). The key novelty lies in modeling P2G and CAES purely for price-driven electrical arbitrage within a retailer's framework, without introducing additional thermal or gas loads, thus maintaining model compatibility while enhancing operational flexibility. Unlike conventional applications, in this work both units are modeled solely as electrical storage layers to enhance flexibility and enable price arbitrage under fixed, Time-of-Use (TOU), and real-time pricing schemes. Surplus renewable generation can be stored either as synthetic gas in the P2G system or as compressed air in the CAES unit, both of which are later converted back into electricity during high-price periods. The proposed extended model improves operational efficiency without introducing additional heat or gas loads. Simulation results show that integrating P2G and CAES reduces total operational cost by 4.5%, increases renewable utilization by 10%, and enhances the ability to shift consumption away from expensive hours.

Keywords: Compressed Air Energy Storage; Demand Response Program; Groundwater Resources; Multi-objective Optimization; Power-to-Gas; Pricing Electricity Sales; Renewable Energy Resources.

1 Introduction

The electricity industry during the past decades has faced restructuring from a monopolistic structure into a competitive one. The restructuring process started in some countries first in the production sector and in some others, such as India, in the distribution sector. In Iran, this sector has become competitive since November 2003 while future strategies include the introduction of competition into the retail sector. In a fully competitive retail market, all consumers are allowed to choose their electricity retailer [1]. The retail market for electricity is the place where retailers purchase from the wholesale market or from other producers, such as distributed generation or energy exchanges. This purchase may be in the form of a half-hourly single rate or bilateral contract. In return, retailers sell the electricity to residential, industrial, and agricultural consumers through term contracts that can range from 1, 2, 3, 6, to 12 months, whose prices are monitored by the regulator[2]. Retailers, among other responsibilities, are required to do demand forecasting, buy energy from the wholesale market, compete with other suppliers, do billing, and protect consumer rights. They are also supposed to involve consumers in demand management programs, perform periodic meter testing, and provide related services to the consumers [3]. Customers in the electricity retail market are of two types: Eligible customers: These customers have the freedom to buy electricity directly from the wholesale or retail market. Non-eligible customers: These customers must purchase their electricity from their local retailer [4].

Some of the benefits that can be brought to consumers by the electricity retail market are lower prices due to competition, freedom to choose suppliers, better services, and demand management [1-4]. The retailer should determine an appropriate selling price in order to maximize profit. Besides, PEVs [2], HSSs [3], and water management systems [5] can be utilized to provide more flexibility and profitability in energy management. In [6], a multi-stage stochastic optimization model is developed considering uncertainties in electricity prices and loads. Mixed-integer-linear-programming provides an effective and adaptable solution framework by addressing the problem's nonlinearity[7]. In [8], a stochastic programming model determines the electricity selling prices to customers based on time-of-use rates. An optimal price offer strategy for the customers, with the objective of maximizing retailer profit, is proposed in [9,10]. In [11], an optimal demand function for retailers in the electricity market is derived. In [12,13], a robust bi-level optimization method for electricity sales is presented. One important way to address the erratic behavior of renewable energy sources and boost the efficiency of the energy system is through demand response programs [14]. The short-term forecasting methods are categorized into two major groups: artificial intelligence and traditional approaches. AI methods, particularly neural networks, have higher accuracy and better adaptability to real nonlinear data for short-term forecasting [15]. Several studies have focused on the stochastic management of energy hubs. For instance, “Stochastic electrical and thermal energy management of energy hubs integrated with demand response programs and renewable energy: A prioritized multi-objective framework” proposes a multi-objective stochastic framework in which the uncertainties of renewable generation and demand response are incorporated at the energy hub level. This approach highlights the importance of scenario-based modeling in enhancing the reliability and flexibility of multi-carrier energy systems[16]. The integration of energy and water infrastructures has also been a challenging research area. The study “Multi-criteria dispatch optimization of a community energy network with desalination: Insights for trading off cost and security of supply” addresses this challenge by proposing a multi-criteria dispatch model that balances the trade-off between economic cost and supply security in community energy networks with desalination units. The results emphasize the significance of considering both economic and reliability objectives simultaneously, which is also relevant to our research in managing water resources[17]. In contrast to our previous works [16], [19] which focused on energy hubs and basic retailer models with conventional storage, this paper specifically introduces P2G and CAES as dedicated electrical storage layers purely for price arbitrage, creating a novel synergy that enhances flexibility without complicating the system with multi-energy couplings. In the context of multi-microgrids, “Optimizing Stochastic Energy Management in Multi-Microgrid Systems Considering Energy Efficiency Improvement Strategies: A Multi-Objective Approach” develops a stochastic multi-objective framework that integrates energy management with energy efficiency improvement strategies. This study demonstrates how combining uncertainty modeling with multi-objective optimization can significantly enhance the performance and reliability of multi-microgrid systems, which shares similarities with the proposed structure in this work[18]. At the electricity retailing level, the work “Management of Renewable Energy Resources and Demand Response in Electricity Retailers with the Presence of Water Systems” investigates the joint management of renewable resources, demand response programs, and groundwater extraction. Although the main focus of this study is on electricity retailers, its insights into electricity pricing and water system management can provide useful references for developing our proposed model, particularly in the integration of water resources[19]. Recent studies have advanced the integration of storage technologies in energy systems. [20] demonstrated the efficacy of CAES in wind-integrated systems for energy shifting and reliability enhancement. Similarly, [21] explored P2G technology in multi-energy systems, highlighting its role in converting excess electricity to hydrogen. However, these approaches primarily focus on multi-carrier energy hubs, introducing complex interactions between electricity, gas, and heat networks [22]. In the context of retailers, previous research has focused on conventional storage and demand

response [19, 23], but the synergistic potential of P2G and CAES as dedicated electrical storage layers for pure price arbitrage remains unexplored. This gap is particularly salient given the need for cost-effective flexibility solutions in smart grids with high renewable penetration.
Research on electricity retailers has looked at many topics, but using new storage systems mainly for buying low and selling high needs more work. Past papers about EVs and hydrogen storage show they help with demand response and renewables. But we don't know enough about using P2G and CAES together for this price arbitrage purpose.Also, when water and energy systems are studied together, the main focus is usually money. Problems like using too much groundwater are not considered much. Heavy groundwater use from high-energy desalination can cause land to sink and water quality to get worse. This paper tries to fill these gaps with a new method that:
- Gets retailers the most profit through smart pricing and storage use
- Reduces groundwater pumping to protect the environment
- Adds P2G and CAES as special electricity storage for better price trading.

The main contributions of this paper are:
1. Integration of two advanced storage technologies (P2G and CAES) as dedicated electrical storage layers for price arbitrage.
2. Development of a multi-objective framework that simultaneously addresses retailer profit maximization and groundwater conservation.
3. Application of neural networks for forecasting uncertain parameters due to their proven effectiveness in handling nonlinear time-series data.
4. Comprehensive evaluation under three pricing schemes, demonstrating the superiority of real-time pricing.
5. Quantitative analysis showing enhanced system flexibility and improved renewable energy utilization.

Structure of the Article:
The mathematical model in Section 2 is proposed by formulating the objective functions and system physical constraints, conducting uncertainty modeling, and proposing a multi-objective decision-making model. The performance evaluation of the model through case studies is done in Section 3. Section 4 discusses the results and presents the future directions of the research.

2 Problem Modeling

2.1 Modeling the cost of the Bilateral contracts

The cost of the energy purchased through bilateral contracts is formulated by Eq. (1), and the minimum and maximum amounts of energy purchased are described by Eq. (2). Eq. (3) shows the sum of purchased energy [24].

$$C_B = \sum_{b}^{B} \sum_{t=1}^{T} \lambda_{b,t} P_{b,t} \tag{1}$$

$$P_b^{\min} S_b \prec P_{b,t} \prec P_b^{\max} S_b \tag{2}$$

$$P_t^{BC} = \sum_{b=1}^{B} P_{b,t} \tag{3}$$

where P_t^{BC} is the total power from bilateral contracts at time t.

2.2 Modeling the cost of the pool market

The cost of energy purchased from the pool market is calculated by Eq. (4) [25]:

$$C_p = \sum_{s=1}^{S} P_s \times \sum_{t=1}^{T} \lambda_{t,s} P_{t,s}^{p} \tag{4}$$

where C_p is total pool market cost, P_s is scenario probability, $\lambda_{t,s}$ is pool price, and $P_{t,s}^{p}$ is power from pool market.

2.3 Modeling the operating cost of DG units

DG units are modeled by a piecewise linear model. Eq. (5) [25] models the cost of purchased energy from DG units. Besides, the purchased energy from DG units is restricted by Eqs. (6) and (7). Eqs. (8) and (9) show the upper and lower ramp rates, respectively. Nonlinear minimum and maximum duration for upper and lower ramp rates are modeled using auxiliary variables Up(i,j) و Dn(i,j).

$$C_{DG} = \sum_{s=1}^{S} P_s \times \sum_{t=1}^{T} \sum_{j=1}^{J} \sum_{h=1}^{H} S_{j,h}^{DG} P_{j,h,t,s}^{DG} \tag{5}$$

$$0 \le P_{j,h,t,s}^{DG} \le P_{j,h}^{\max} - P_{j,h-1}^{\max} \tag{6}$$

$$0 \le P_{j,1,t,s}^{DG} \le P_{j,1}^{\max} \tag{7}$$

$$\sum_{h=1}^{H} P_{j,h,t,s}^{DG} - \sum_{h=1}^{H} P_{j,h,t-1,s}^{DG} \le R_j^{Up} \times U_{j,t}^{DG} \tag{8}$$

$$\sum_{h=1}^{H} P_{j,h,t-1,s}^{DG} - \sum_{h=1}^{H} P_{j,h,t,s}^{DG} \le R_j^{Down} \times U_{j,t-1}^{DG} \tag{9}$$

$$U_{j,t}^{DG} - U_{j,t-1}^{DG} \le U_{j,t+Up_{j,i}}^{DG} \tag{10}$$

$$U_{j,t-1}^{DG} - U_{j,t}^{DG} \le U_{j,t+Dn_{j,i}}^{DG} \tag{11}$$

2.4 Modeling of wind and solar systems

For a variable-speed wind turbine, the relationship between power and wind speed is based on the information provided in [26].
Similarly, the power extractable from a photovoltaic system is calculated using the data provided in [26].

2.5 Hydrogen storage system modeling

In the electrolyzer model, the power is utilized to generate hydrogen and store it in hydrogen tanks whenever there is a low demand for it. The minimum and maximum power consumed can be analyzed using Eqs. (12) and (13), respectively. The maximum quantity of hydrogen produced is given by Eq. (14). Lastly, Eq. (15) shows that hydrogen generation is a function of the power input to the electrolyzer [3].

$$P_{t,s}^{EL} \le P_{\max}^{EL} \times U_{t,s}^{EL} \tag{12}$$

$$P_{t,s}^{EL} \ge P_{\min}^{EL} \times U_{t,s}^{EL} \tag{13}$$

$$N_{H2,t,s}^{EL} \le N_{H2,\max}^{EL} \times U_{t,s}^{EL} \tag{14}$$

$$N_{H2,t,s}^{EL} = \frac{\eta^{EL} P_{t,s}^{EL}}{LHV_{H2}} \tag{15}$$

The initial hydrogen pressure, minimum, and maximum hydrogen tank pressure are modeled by Eqs. (16) to (18)[3]:

$$P_{t0}^{H2} = P_{initial}^{H2} \tag{16}$$

$$P_{t,s}^{H2} \le P_{\max}^{H2} \tag{17}$$

$$P_{t,s}^{H2} \ge P_{\min}^{H2} \tag{18}$$

In the model of the fuel cell, during peak demand, the stored hydrogen is utilized to generate power. The minimum and maximum hydrogen produced by the fuel cell are depicted in Eq. (19). The hydrogen consumed as shown by Eq. (20) is a function of the power generated by the fuel cell. Lastly, Eqs. (21) and (22) model the minimum and maximum power output from the fuel cell [3].

$$N_{H2,t,s}^{FC} \le N_{H2,\max}^{FC} \times U_{t,s}^{FC} \tag{19}$$

$$N_{H2,t,s}^{FC} = \frac{P_{t,s}^{FC}}{\eta^{FC} LHV_{H2}} \tag{20}$$

$$P_{t,s}^{FC} \le P_{\max}^{FC} \times U_{t,s}^{FC} \tag{21}$$

$$P_{t,s}^{FC} \ge P_{\min}^{FC} \times U_{t,s}^{FC} \tag{22}$$

The fuel cell and electrolyzer cannot work at the same time in the hydrogen storage system. This implies from Eq. (23) that charge/discharge modes could not happen simultaneously. The dynamic pressure model of the hydrogen storage system is expressed as Eq. (24).

$$U_{t,s}^{FC} + U_{t,s}^{EL} = 1 \tag{23}$$

$$P_{t,s}^{H2} = P_{t-1,s}^{H2} + \frac{RT_{H2}}{V_{H2}}(N_{H2,t,s}^{EL} - N_{H2,t,s}^{FC}) \tag{24}$$

2.6 Modeling of a Plug-in Hybrid Electric Vehicle

Eqs. (25)-(31) model the technical constraints of Plug-in Hybrid Electric Vehicles [27]. Eq. (25) shows the initial charge of the vehicle. The charge of the vehicle at each instant is given by Eq. (26). The minimum and maximum charges of the vehicle are modeled by Eq. (27). The energy required for the travel of the vehicle is defined by Eq. (28). Besides, Eqs. (29) and (30) consider the upper and lower limits for the vehicle's charge and discharge power. The binary state of the vehicle is expressed by Eq. (31). It shows that the vehicle cannot charge and discharge at the same time [2].

$$SOC_{t0,v,s} = E_v^0 \tag{25}$$

$$SOC_{t,v,s} = SOC_{t-1,v,s} + \eta_v^c \times Pc_{t,v,s} - \frac{Pd_{t,v,s}}{\eta_v^d} - Ptr_{t,v} \tag{26}$$

$$SOC_v^{\min} \le SOC_{t,v,s} \le SOC_v^{\max} \tag{27}$$

$$Ptr_{t,v} = \Delta D_{t,v} \times \Omega v \tag{28}$$

$$Pc_v^{\min} \times Uc_{t,v,s} \le Pc_{t,v,s} \le Pc_v^{\max} \times Uc_{t,v,s} \tag{29}$$

$$Pd_v^{\min} \times Ud_{t,v,s} \le Pd_{t,v,s} \le Pd_v^{\max} \times Ud_{t,v,s} \tag{30}$$

$$Uc_{t,v,s} + Ud_{t,v,s} = 1 \tag{31}$$

2.7 Power supplied by the retailer

The power provided by the retailer is determined from the following equations. From Eqs. (32)-(35), the power supply for each group of customers in each period is a function of the selling price [12].

$$D(l,t,s) = \sum_{z=1}^{Z} D^{offer}(l,z,t,s) A(l,z,t); \forall l,t,s \tag{32}$$

$$SP(l,t) = \sum_{z=1}^{Z} SP(l,z,t); \qquad \forall l,t \tag{33}$$

$$\begin{aligned} SP^{offer}(l,z-1,t) A(l,z,t) &\le SP(l,z,t) \\ &\le SP^{offer}(l,z) A(l,z,t); \forall l,t \end{aligned} \tag{34}$$

$$\sum_{z=1}^{Z} A\left(l,z,t\right)=1; \qquad \forall l,t \tag{35}$$

2.8 Retailer's Revenue Function

The revenue from the sale of energy to subscribers of group l at time t is calculated as follows [12]:

$$R_R(l,t)=\sum_{s=1}^{S} P_s \times SP(l,t)D(l,t,s) \tag{36}$$

The retailer selects a portion of the customer demand based on the price-quota curve for the customer that is offered to the retailer for energy supply.

2.9 Water system model

The power consumption for water pumping from the well is a function of the flow rate, as defined in Eq. (37) [6]. Desalination is the second method used to supply the system's water requirements. The power consumption for water desalination is described by Eq. (38), while the water produced by the desalination unit is limited by Eq. (39). The physical constraints of the water storage system are given in Eqs. (40) to (44) [28-29]. Eq. (40) describes the water level in the storage system. The admissible water levels are restricted by Eq. (41).. The charging and discharging rates of water are limited by Eqs. (42) and (43). Eq. (44) confirms that the water storage system cannot operate in both charging and discharging modes simultaneously. Finally, Eqs. (45) and (46) are the water balance and electrical power consumed by the water system, respectively [5].

$$P_t^{pw,w}=Q_t^{w,w}LL^{w,w}\frac{g^{w}\rho^{w}}{\eta^{p,w}(3.6\times10^{6})} \tag{37}$$

$$P_t^{d,w}=\eta^{d,w}Q_t^{d,w} \tag{38}$$

$$0\le Q_t^{d,w}\le Q_{\max}^{d,w} \tag{39}$$

$$L_t^{s,w}=L_{t-1}^{s,w}+Q_t^{w,ch}-Q_t^{w,disch} \tag{40}$$

$$0\le L_t^{s,w}\le L_{\max}^{s,w} \tag{41}$$

$$0\le Q_t^{w,ch}\le Q_{\max}^{w,ch}WW_t^{w,ch} \tag{42}$$

$$0\le Q_t^{w,disch}\le Q_{\max}^{w,disch}WW_t^{w,disch} \tag{43}$$

$$0\le WW_t^{w,ch}+WW_t^{w,disch}\le 1 \tag{44}$$

$$Q_t^{w,w}+Q_t^{d,w}+Q_t^{w,disch}=Q_t^{w,ch}+L_t^{wl} \tag{45}$$

$$P_t^{water,w}=P_t^{d,w}+P_t^{pw,w} \tag{46}$$

2.10 Balance of power:

The power balance constraint at any time is calculated by Eq. (47).

$$\begin{aligned}&\sum_{b=1}^{B}P_{b,t}+\sum_{j=1}^{J}\sum_{h=1}^{H}P_{j,h,t,s}^{DG}+P_{t,s}^{P}+P_{t,s}^{wind}+P_{t,s}^{PV}+P_{t,s}^{FC}\\&+\sum_{v=1}^{V}Pd_{t,v,s}+P_{G2P}(t)-P_{P2G}(t)-V^{P}(t)+V^{inj}(t)\\&=\sum_{l=1}^{L}D(l,t,s)+P_{t,s}^{EL}+\sum_{v=1}^{V}Pc_{t,v,s}+P_{t,s}^{water}(t)\end{aligned} \tag{47}$$

2.11 Objective function

The first objective function is to maximize the expected profit of the retailer in the energy market. Revenue to the retailer results from the selling of electricity to customers. On top of that, the retailer's electricity procurement comes from three resources: the shared pool market, bilateral contracts, and distributed generation sources.

The retailer's objective function appears in Eq. (48) and is supposed to be maximized over the constraints modeled between Eqs. (1) through (47).

$$\begin{aligned}&Max\sum_{s=1}^{S}P_s\times\left\{\sum_{t=1}^{T}\sum_{l=1}^{L}SP(l,t)D(l,t,s)\right.\\&\left.-\sum_{t=1}^{T}\lambda_{t,s}P_{t,s}^{P}-\sum_{t=1}^{T}\sum_{j=1}^{J}\sum_{h=1}^{H}S_{j,h}^{DG}P_{j,h,t,s}^{DG}\right\}\\&-\sum_{b=1}^{B}\sum_{t=1}^{T}\lambda_{b,t}P_{b,t}^{P}-\sum_{t=1}^{T}\pi_t^{CAES}V^{inj}(t)-\sum_{t=1}^{T}\pi_t^{ch}P_{P2G}(t)\end{aligned} \tag{48}$$

The volume of freshwater extracted from underground sources is a function of another objective, which is given in Eq. (49).

$$\text{MinEW}^{\text{water}}=\sum_{t}Q_t^{w,w} \tag{49}$$

2.12 Uncertainty modeling

To model the uncertainty of the pool market, the predicted distribution curves of demand, temperature, solar radiation, and wind speed have been divided into five segments, each with one standard deviation. The value for standard deviation is taken to be 10%. The uncertainty modeling takes the parameters from the deterministic case as average values. For the five uncertain parameters considered in this study, it is assumed that there is one scenario for each; therefore, a total of 55 scenarios are taken into consideration. The initial scenario set comprised 55 scenarios, rendering the optimization problem computationally prohibitive. To mitigate this, the Kantorovich distance-based scenario reduction technique was applied [29]. This method systematically eliminates scenarios with low probabilities and high similarity to others, thereby preserving the statistical representation of uncertainties while enhancing computational tractability. The final set of five scenarios was selected to capture the most probable and distinct realizations of uncertain parameters, including combinations of high renewable generation with low electricity prices, low renewable output with high prices, and expected average conditions.

2.13 Determining the selling price of electricity

The basis of electricity prices is considered based on a time index with three modes: Real-time pricing, Fixed-pricing, Time-of-use Pricing.

2.14 Demand Response Program Modeling

Eqs. (50) to (53) represent the new demand in the presence of a demand response program. It is worth noting that in the demand response program, part of the load can be shifted to a different time period. However, the total load over the period T remains constant. Eq. (50) shows the new load demand. Eqs. (51) and (52) indicate that the increase or decrease in the load is limited by a variable , which is considered to be 20%. Additionally, Eqs. (36) and (48) are also adjusted to account for the new demand [26].

$$Ddr(l,s,t) = D(l,s,t) + DRP(l,s,t) \tag{50}$$

$$DRP(l,s,t) \le +DRP^{\max} \times D(l,s,t) \tag{51}$$

$$DRP(l,s,t) \ge -DRP^{\max} \times D(l,s,t) \tag{52}$$

$$\sum_{t=1}^{T} DRP(l,s,t) = 0 \tag{53}$$

2.15 Power-to-gas and CAES Modeling

In the proposed extended model, two additional storage technologies are incorporated into the electricity layer: (i) a P2G unit connected to a gas storage tank and an on-site gas-to-power conversion process, and (ii) a CAES unit with a compressed air storage reservoir. Both units are charged during low-price or surplus renewable periods and discharged to supply electricity during high-price intervals. No external gas or heat demands are considered, maintaining compatibility with the original water–energy retailer framework. In the following, (54)-(60) models the operation of the CAES technology[29].

$$V^{inj}(t) = \alpha^{inj} P_{CAES}(t) \tag{54}$$

$$P_{C,S}(t) = \alpha^{P} V^{P}(t) \tag{55}$$

$$V_{\min}^{inj} u^{inj}(t) \le V^{inj}(t) \le V_{\max}^{inj} u^{inj}(t) \tag{56}$$

$$V_{\min}^{P} u^{P}(t) \le V^{P}(t) \le V_{\max}^{P} u^{P}(t) \tag{57}$$

$$u^{inj}(t) + u^{P}(t) \le 1 \tag{58}$$

$$A(t+1) = A(t) + V^{inj}(t) - V^{P}(t) \tag{59}$$

$$A^{\min} \le A(t) \le A^{\max} \tag{60}$$

Eqs. (54) and (55) indicate the energy import and export in the CAES unit. The imported and exported energy in the CAES unit is limited by (56) and (57) respectively. The energy level of the CAES unit is obtained by (59). Furthermore, the capacity of the CAES unit is limited by (60). The P2G system is modeled as follow[29]:

$$GS(t) = GS(t-1) + G_{P2G}^{ch}(t) - G_{P2G}^{dis}(t) \tag{61}$$

$$GS^{\min} \le GS(t) \le GS^{\max} \tag{62}$$

$$G_{P2G}^{ch,\min} \le G_{P2G}^{ch}(t) \le G_{P2G}^{ch,\max} \tag{63}$$

$$G_{P2G}^{dis,\min} \le G_{P2G}^{dis}(t) \le G_{P2G}^{dis,\max} \tag{64}$$

$$G_{P2G}^{ch}(t) = \eta_{P2G} P_{P2G}(t) \tag{65}$$

$$G_{P2G}^{dis}(t) = \eta_{G2P} P_{G2P}(t) \tag{66}$$

$$0 \le P_{G2P}(t) \le P_{G2P}^{\max} \tag{67}$$

$$0 \le P_{P2G}(t) \le P_{P2G}^{\max} \tag{68}$$

Constraint (60) shows the charge level of the P2G system. The charge level of the P2G system is limited by (61). Charging and discharging the P2G system are limited by (62) and (63) respectively. Moreover, the energy conversion in the P2G system is modeled by (64) and (67).

2.16 Multi-objective decision-making framework

The energy system has been analyzed from the point of view of optimal performance both from ecosystem and economic points of view. In order to get the best design, a multi-objective decision-making framework is utilized. To change the multi-objective to a single-objective problem, the normalized weighted sum approach has been proposed. This technique has the advantage of pointing out one solution. For instance, the model of an optimization objective function, with FIdeal and FNadir representing the best and the worst solutions of objective I, respectively, is defined in Eq. 69[30,31]:

$$Min\left(W_1^g \frac{F_1}{F_1^{Nadir} - F_1^{Ideal}} + W_2^g \frac{F_2}{F_2^{Nadir} - F_2^{Ideal}}\right) \quad (69)$$
$$\sum_i W_i^g = 1, \qquad W_i^g \in (0,1)$$

where W_1^S and W_2^S are weights for profit and water objectives, F_1^{Ideal} and F_1^{Nadir} are best/worst values for profit, F_2^{Ideal} and F_2^{Nadir} are best/worst values for water usage.

2.17 Solution Approach

The model is solved using mixed-integer linear programming. The solution process follows these steps:
First, forecasting methods provide input data for uncertain parameters including market prices and renewable energy output.
Next, multiple scenarios are generated to represent different possible conditions in the electricity market and renewable generation.
The Kantorovich technique then reduces these scenarios to a manageable number while maintaining their key characteristics.
The main optimization problem is solved using commercial optimization software, determining the optimal operation of all storage systems and power procurement decisions.
Finally, the weighted-sum method converts the multi-objective problem into a single optimization that balances economic and environmental goals.
The output includes detailed scheduling for all energy storage units and optimal electricity prices for different customer groups.

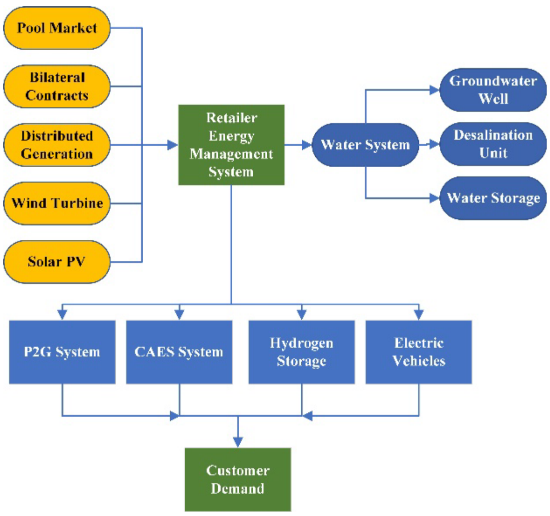

Fig. 1. Schematic of the proposed system.

3 Simulation Results

In this section, four case studies are considered to illustrate the result of determining the selling price under three methods, including time-of-use pricing, fixed-pricing, and real-time pricing. In addition, by applying the demand response program, the results of the four cases under these three methods are evaluated. Finally, a water system is considered for the fourth case.
In [25], daily demand has been considered in three load levels: mid-peak, off-peak, and peak periods. Moreover, the amount of twelve bilateral contracts including the upper and lower limit energy and price in connection with the peak and all load levels have been given in Table 1. The Distributed generation units specification and the parameters of wind turbine and PV have been given in [25]. At last, [27] and [3] have provided the parameters of HSSs and PEVs, respectively. Moreover, Fig. 2 depicts the relevance between the sales price and the demand of customer groups supplied by retailers. In Fig. 2 there are 100 steps as a stepwise quota price curve for every customer. Whereas, the forecasted shared market price and also the retailer load curve for the time periods can be shown from [21].
Four case studies are studied under three types of pricing techniques that are mentioned, as outlined in Table 2, in order to analyze the impact of HSSs and PEVs on energy management and determination of optimal sales price.
In the first method, the selling price is presumed to be fixed in all periods of time; hence, the first objective function is maximized with consideration of constraints and also incorporating HSSs and PEVs.
The results of the simulation for fixed-pricing are shown in Table 3. It can be seen from Table 3 that the retailer's profit increases by 3.75%, 2.75%, and 11.54% in cases 2, 3, and 4, respectively, using energy storage systems and electric vehicles. It must be mentioned that the increase in profit in cases 2 and 3 is only because of the use of HSSs and PEVs in energy management. The higher synergy between the joint impacts of HSSs and PEVs together in Case 4 thus produces a much larger profit as compared to Cases 1, 2, and 3.
The fixed sales prices for commercial, residential, and industrial customers are also shown in Table 3. Due to the use of HSSs and PEVs in cases 2, 3, and 4, the fixed sales prices for these customer groups slightly increased because of the increase in the expected final profit of the retailer. This is favorable for retailers but appropriate for end customers.

Table 1. Specifications of Bilateral Contracts.

Contract Number	Load Level	Max (kW)	Min (kW)	Price (USD/kWh)
1	Three-Level	50	15	0.04
2	Peak	40	10	0.043
3	Three-Level	50	15	0.05
4	Peak	40	10	0.048
5	Three-Level	70	25	0.032
6	Peak	60	20	0.041
7	Three-Level	70	25	0.051
8	Peak	60	20	0.048
9	Three-Level	70	25	0.043
10	Peak	60	20	0.058
11	Three-Level	70	25	0.052
12	Peak	60	20	0.057

The total amount of purchased power from the shared market can be depicted in Fig. 3. The charging/discharging percentages of the electric vehicles have been given in Fig. 4. The storages of the hydrogen are shown in Fig. 5.

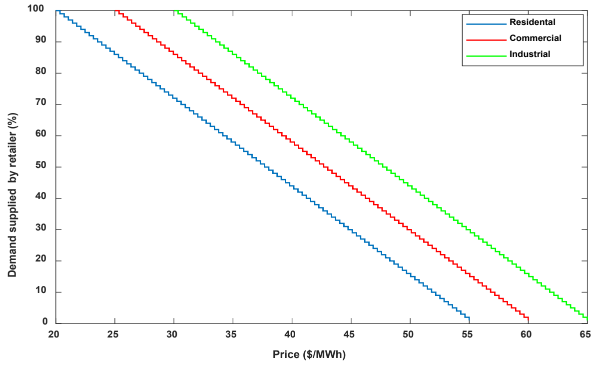

Fig. 2. Price-quota curves.

Table 2. Classification of three methods under four case studies for evaluating model.

Methods	Method 1		Method 2		Method 3	
	Fixed Pricing		Time-of-Use Pricing		Real-Time Pricing	
Scenarios	PEVs	HSSs	PEVs	HSSs	PEVs	HSSs
Scenario 1						
Scenario 2	✓		✓		✓	
Scenario 3		✓		✓		✓
Scenario 4	✓	✓	✓	✓	✓	✓

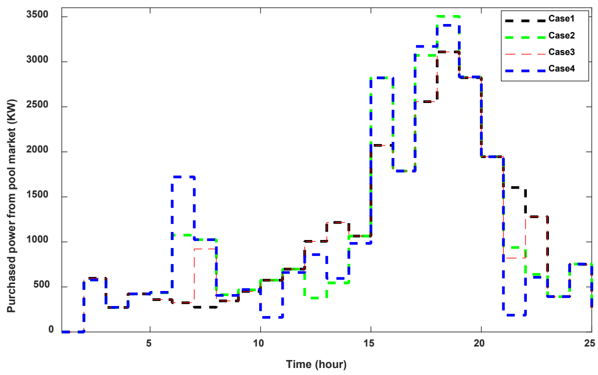

Fig. 3. Power from the pool market in fixed-pricing strategy.

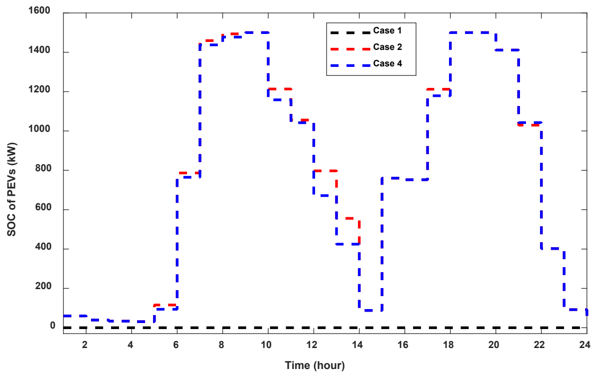

Fig. 4. PEVs' condition in fixed-pricing strategy.

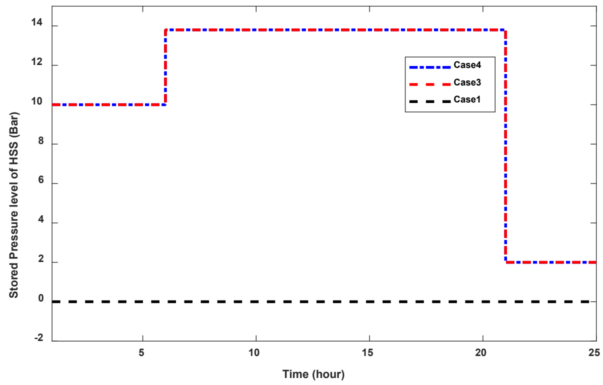

Fig. 5. HSSs' Stored pressure level in fixed-pricing strategy.

The retailer sets the off-peak, mid-peak, and peak sales prices under the time-of-use pricing model. On the other hand, time-of-use pricing is close to reality, unlike fixed-pricing.

It is reflected in Table 3 that the profit of the retailer increases by 3.81%, 2.34%, and 6.48% in cases 2, 3, and 4 respectively, due to the use of PEVs and HSSs. Similar to approach 1 (Fixed-pricing), positive impacts brought by PEV and HSS utilization in case studies 2, 3, and 4 drive higher profits than in first case.

Furthermore, the time-of-use sales price for off-peak, mid-peak, and peak intervals for residential, commercial, and industrial customers can be obtained from Table 3. Based on this table, it is found that the time-of-use sale price in Case 4 is less than those in Cases 1, 2, and 3. This reduction comes because of the application of HSSs and PEVs while increasing the expected final profit of the retailer. Therefore, unlike the fixed-pricing strategy, these results benefit the retailer and the end customers.

Fig. (6) presents the purchased power from the shared market. Fig. (7) presents the percentages of charge and discharge for an electric vehicle. The state of charge profiles in Fig. (7) demonstrate effective load shifting through PEV management. Vehicles charge during off-peak hours (periods 1-6) when electricity prices are lowest, and discharge during peak demand hours (periods 18-21), reducing the retailer's procurement costs during high-price intervals. Fig. (8) shows the hydrogen storage pressure dynamics, indicating optimal operation of the electrolyzer during low-price periods and fuel cell utilization during peak hours. The system maintains pressure within safe operational limits while supporting peak shaving.

The determination of sales prices by using real-time pricing is closer to reality in the smart grid environment. Hence, the first objective function (Eq. 48) should be maximized considering constraints (1) to (47) and (49). Simultaneously, the real-time price needs to be determined by the retailer based on constraint (49). Table 3 presents real-time pricing simulation results using and not using electric vehicles and storage systems (Cases 1 to 4). In this table, the profits of the retailer using energy storage systems and electric vehicles were higher than in those cases where their use was not considered by up to 3.59%, 2.51%, and 6.1% for Cases 2, 3, and 4, respectively.

Similar to previous strategies, electric vehicles and hydrogen storage systems provide more positive results in cases 2, 3, and 4 in order to gain higher profits than the first case. It is observed from results that the first objective function in real-time pricing for the last case has a better result among the different approaches and cases. This is so because the retailer fixes a sales price via real-time pricing and smart management of PEV charging/discharging and the usage of HSS hence yielding more profits. Fig. (11) shows in every time period, how real-time sale prices for commercial, residential, and industrial clients change. It is seen from these figures that the real-time sales price in the presence of smart management of PEV charging and discharging and hydrogen storage systems is lower than when such smart management is absent.

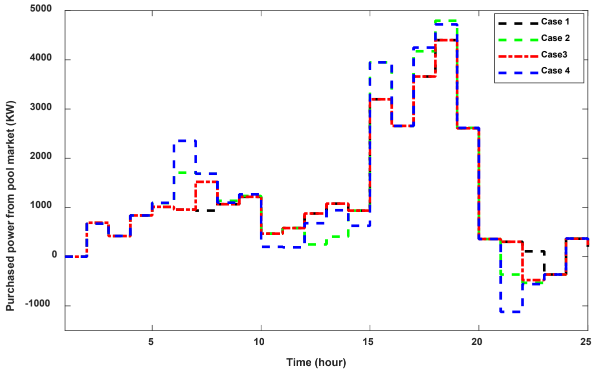

Fig. 6. Utilizing pool market power in a time-of-use pricing strategy.

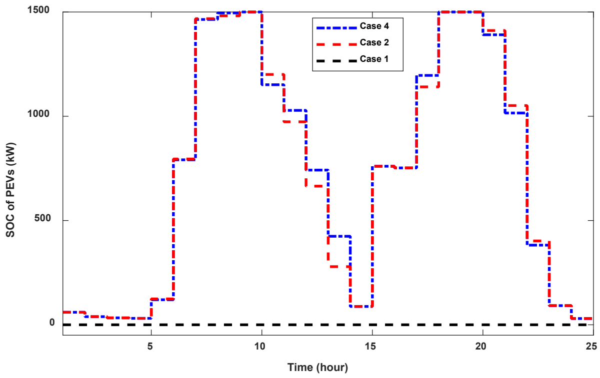

Fig. 7. Time-of-use pricing strategy for PEVs' SOC.

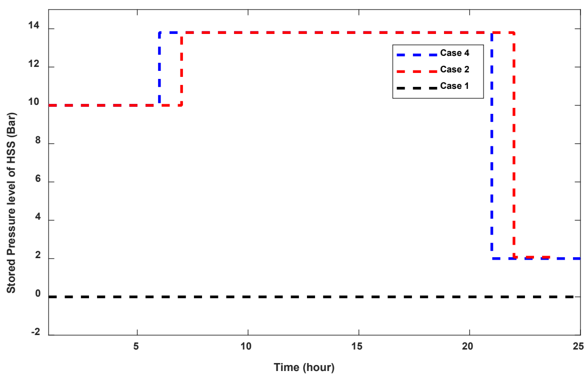

Fig. 8. HSSs' Stored pressure level in time-of-use pricing strategy.

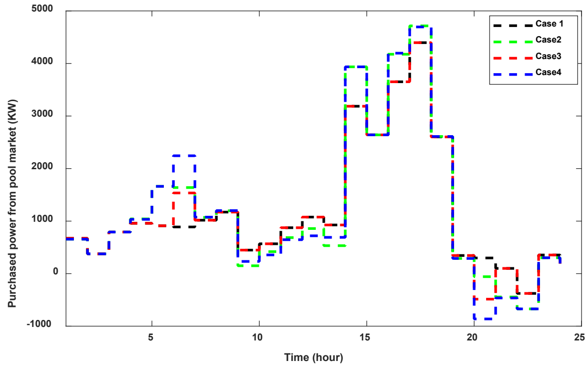

Fig. 9. Utilizing pool market power in a real-time pricing strategy.

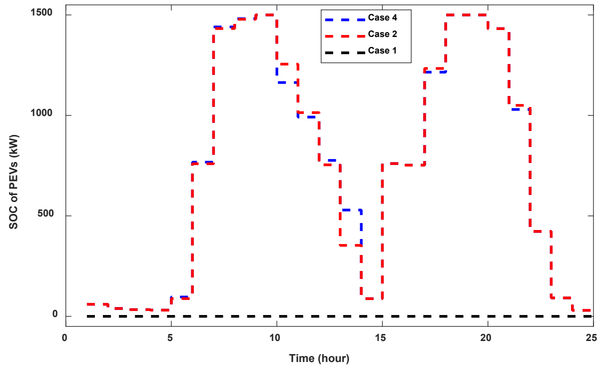

Fig. 10. real-time pricing strategy for PEVs' SOC.

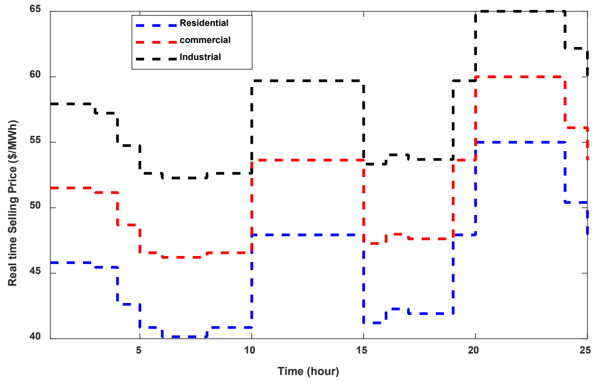

Fig. 11. Selling prices in real time for various client types.

These results benefit the retailer and the end customers as well. So, smart management of PEV charging/discharging along with HSS usage reduces sales prices, especially at peak periods. That benefits the customer; at the same time, this is useful to the retailer also, because expected profit increases. This strategy satisfies both the retailer and the customer.

Therefore, compared to fixed-pricing and time-of-use pricing strategies, the outcomes of real-time pricing are better for the retailer and the final consumers. Determining the sales price by real-time pricing and utilizing smart management of PEV charging and discharging and HSS use is closer to reality and provides higher expected profit for the retailer.

In the real-time pricing method, the load supplied by the retailer for customers is presented in Fig. (9). Fig. (9) indicates that optimality of the load profile in the last case is more than others because during peak periods the supplied load is higher, which is desirable for end customers. Thus, the expected profit in the last case is more than in other cases, that could be appropriate to the retailer.

Table 3 also provides a comparison of all studied cases under different strategies. It is evident that the real-time pricing strategy yields the highest profit for the retailer. Electricity sales prices under the time-of-use tariff strategy decrease compared to the fixed-pricing strategy (except during peak periods). As a result, both the retailer and the consumer benefit. Similarly, with real-time pricing, the average electricity sales price also decreases. Consequently, energy storage systems and electric vehicles show a better impact under the real-time pricing strategy, benefiting both consumers (through reduced electricity sales prices) and the retailer (through increased expected profit).

Table 3. Comparison of the Results from All Pricing Strategies for the Four Mentioned Studies.
Units: Expected Profit, Revenue, Cost (USD); Electricity Prices (USD/MWh).

Pricing Strategy	Case 1	Case 2	Case 3	Case 4
Fixed Tariff				
Expected Profit	1235.61	1284.18	1269.62	1318.19
Profit Increase	0	3.93	2.75	11.54
Expected Revenue	2505.56	2505.56	2505.561	2505.56
Total Expected Cost	1269.95	1221.38	1235.941	1187.37
Electricity Prices				
Residential Consumer	46.515	46.86	46.86	46.87
Commercial Consumer	52.93	52.93	52.93	52.93
Industrial Consumer	58.99	58.99	58.99	58.99
Time-of-Use Tariff				
Expected Profit	1272.83	1321.41	1302.68	1355.42
Profit Increase	0	3.81	2.34	6.48
Expected Revenue	2465.71	2465.71	2465.71	2465.71
Total Expected Cost	1192.88	1144.3	1162.67	110.286
Electricity Prices				
Off-Peak (Residential)	42.273	42.273	42.273	42.273
Mid-Peak	44.7748	44.7748	44.7748	44.7748
Peak	50.404	50.404	50.404	50.404
Off-Peak (Commercial)	48.33	48.33	48.33	48.33
Mid-Peak	50.81	50.81	50.81	50.81
Peak	56.465	56.465	56.465	56.465
Off-Peak (Industrial)	54.394	54.394	54.394	54.394
Mid-Peak	56.869	56.869	56.869	56.869
Peak	62.525	62.525	62.525	62.525
Real-Time Tariff				
Expected Profit	1353.04	1401.62	1387.059	1435.632
Profit Increase	0	3.59	2.51	6.1
Expected Revenue	2514.06	2671.573	2504.64	2514.09
Total Expected Cost	1160.59	1269.953	1126.582	1078.379

Table 4 highlights the role of fuel cells and hydrogen storage systems in managing the electricity retailer's energy in the presence of renewable energy sources, electric vehicles, and demand response (DR) programs. The results demonstrate the positive impact of DR on increasing the retailer's profit across all strategies. Comparing the overall results with the DR program, it is clear that the highest profit for the retailer is achieved under the real-time pricing tariff in the presence of DR.

Table 5 illustrates the impact of incorporating the water system into the problem (only for case 4), which transforms the objective function into a multi-objective one. It is observed that the addition of water, due to the increased load, reduces the expected profit across all three pricing strategies. Additionally, Fig. 12 shows the water resource level, which is higher under the real-time pricing strategy.

Table 4. Expected Profit of All Pricing Strategies for the Four Mentioned Studies Considering the Demand Response Program.
Units: Expected Profit (USD).

Pricing Strategy	Case 1	Case 2	Case 3	Case 4
Fixed Tariff	1238.54	1336.653	1335.97	1383.48
Time-of-Use	1341.5	1391.71	1345.28	1435.632
Real-Time Pricing	1367.49	1416.96	1469.666	1491.94

Table 5. Comparison of the Results from All Pricing Strategies for the Fourth Study Considering the Demand Response Program and the Water System.
Units: Expected Profit (USD); Extracted Water Volume (L).

Pricing Strategy	Expected Profit	Extracted Water Volume (Liters)
Fixed Tariff	1243.736	46
Time-of-Use	1246.325	46
Real-Time Pricing	1351.465	46

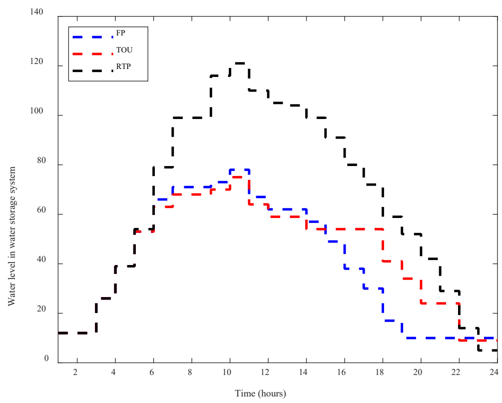

Fig. 12. Water Storage Levels in Three Strategies.

Finally, with the addition of the gas network and gas storage devices to the fourth case, as well as changes in the balance equation and taking into account the demand response programs, the expected profit amount in the three tariffs will be as shown in Table 6. It is observed that the addition of gas, reduces the expected profit across all three pricing strategies. A quantitative analysis confirms the specific contribution of P2G and CAES integration. As demonstrated in Table 6, adding P2G and gas storage capabilities to the system increases expected profit across all pricing schemes: from 1243.736$ to 1292.795$ under fixed pricing (3.9% improvement), from 1246.325$ to 1302.670$ under time-of-use pricing (4.5% improvement), and from 1351.465$ to 1414.598$ under real-time pricing (4.7% improvement). Additionally, the integration of P2G and CAES enables a 10% increase in renewable energy utilization by storing surplus renewable generation that would otherwise be curtailed. These results highlight the significant value of P2G and CAES technologies in enhancing retailer profitability through effective price arbitrage. Fig. 13 and Fig. 14 show the operation of the CAES unit and P2G system in Three Strategies. The results show that the CAES unit and P2G are appropriate for energy arbitrage between hours. In this regard, the system operator imports energy in the P2G and CAES units at the high energy price hours and exports the stored energy at the lower price hours.

Table 6. Expected Profit of All Pricing Strategies for the Fourth Study Considering the Demand Response Program, the Water System and gas storage.
Units: Expected Profit (USD).

Pricing Strategy	Expected Profit (case4+water)	Expected Profit (case4+water+gas)
Fixed Tariff	1243.736	1292.795
Time-of-Use	1246.325	1302.670
Real-Time Pricing	1351.465	1414.598

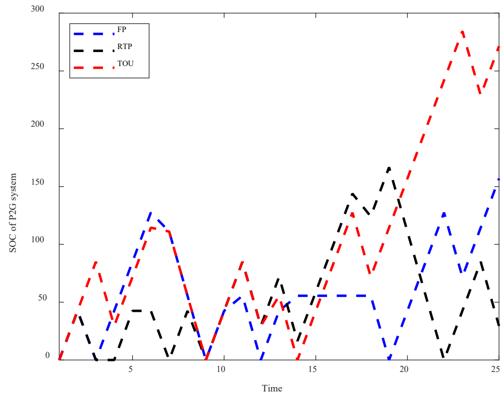

Fig. 13. The SOC of the P2G unit in Three Strategies.

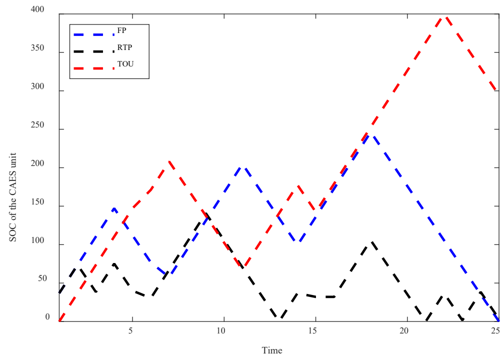

Fig. 14. The SOC of the CAES unit in Three Strategies.

4 Conclusion

This study investigated the operation of a smart grid integrating Power-to-Gas (P2G) and Compressed Air Energy Storage (CAES) with renewable energy resources and demand response programs. The framework was evaluated under fixed, time-of-use, and real-time pricing schemes. Surplus electricity from renewable generation is stored as synthetic gas or compressed air and later converted back to electricity during high-price periods, allowing for effective price arbitrage. Uncertainties in renewable output and demand were addressed using a scenario-based probabilistic approach. The results indicate that real-time pricing offers the most favorable performance, reducing total operational costs by 4.5% and increasing renewable energy utilization by 10%. The integration of P2G and CAES enhances system flexibility and peak-load management compared to conventional configurations without advanced storage. Demand response programs further improve cost efficiency across all pricing strategies. Despite its contributions, this study has some limitations that suggest directions for future work. The model does not consider the capital investment costs of P2G and CAES systems, which could affect economic feasibility analysis. Furthermore, the solution approach, while effective, could be enhanced with AI-driven techniques such as deep reinforcement learning for real-time adaptive control. Future research will also explore the expansion of this framework to fully coupled multi-energy systems including thermal and gas networks, and investigate the integration of hydrogen storage systems with the proposed P2G-CAES configuration for long-term seasonal storage.

Disclosure of Potential Conflicts of Interest

The Authors declare that there is no conflict of interest

Reference

[1] S. Nojavan, B. Zare, and K. Zare, "Strategic decision-making for electricity retailers in the competitive market: A comprehensive review," Energy Strategy Reviews, vol. 47, p. 101102, 2023, doi: 10.1016/j.esr.2023.101102.

[2] H. Morais, T. Sousa, J. Soares, P. Faria, and Z. Vale, "Distributed energy resources management using plug-in hybrid electric vehicles as a fuel-shifting demand response resource," Energy Conversion and Management, vol. 97, pp. 78–93, 2015, doi: 10.1016/j.enconman.2015.03.002.

[3] G. Cau, D. Cocco, M. Petrollese, S. K. Kær, and C. Milan, "Energy management strategy based on short-term generation scheduling for a renewable microgrid using a hydrogen storage system," Energy Conversion and Management, vol. 87, pp. 820–831, 2014, doi: 10.1016/j.enconman.2014.07.078.

[4] S. Feuerriegel and D. Neumann, "Measuring the financial impact of demand response for electricity retailers," Energy Policy, vol. 65, pp. 359–368, 2014, doi: 10.1016/j.enpol.2013.10.017.

[5] M. J. V. Pakdel, F. Sohrabi, and B. Mohammadi-Ivatloo, "Multi-objective optimization of energy and water management in networked hubs considering transactive energy," Journal of Cleaner Production, vol. 266, p. 121936, 2020, doi: 10.1016/j.jclepro.2020.121936.

[6] M. S. Javadi, A. E. Nezhad, and J. P. S. Catalão, "Stochastic optimization for electricity retailers in competitive markets with renewable energy sources and energy storage systems," Electric Power Systems Research, vol. 216, p. 109024, 2023, doi: 10.1016/j.epsr.2022.109024.

[7] M. R. Masoudi, M. Haghighi, and M. R. Behbahani, "Optimal operation of solar energy system integrated with energy storage

systems," Power, Control, and Data Processing Systems, vol. 1, no. 1, 2024, doi: 10.30511/PCDP.2024.718345.

[8] M. M. Bidgoli, "Stochastic energy scheduling in multiple microgrid systems considering independence index and energy not supply index," Iranian Journal of Energy, vol. 27, no. 2, pp. 67-87, 2024.

[9] M. Charwand and Z. Moshavash, "Midterm decision-making framework for an electricity retailer based on information gap decision theory," International Journal of Electrical Power and Energy Systems, vol. 63, pp. 185–195, 2014, doi: 10.1016/j.ijepes.2014.05.073.

[10] N. Mahmoudi-Kohan, M. P. Moghaddam, M. K. Sheikh-El-Eslami, and E. Shayesteh, "A three-stage strategy for optimal price offering by a retailer based on clustering techniques," International Journal of Electrical Power and Energy Systems, vol. 32, no. 10, pp. 1135–1142, 2010, doi: 10.1016/j.ijepes.2010.06.006.

[11] M. Hajati, H. Seifi, and M. K. Sheikh-El-Eslami, "Optimal retailer bidding in a DA market—A new method considering risk and demand elasticity," Energy, vol. 36, no. 2, pp. 1332–1339, 2011, doi: 10.1016/j.energy.2010.10.059.

[12] W. Wei, F. Liu, and S. Mei, "Energy pricing and dispatch for smart grid retailers under demand response and market price uncertainty," IEEE Transactions on Smart Grid, vol. 6, no. 3, pp. 1364–1374, 2014, doi: 10.1109/TSG.2014.2384489.

[13] M. Khojasteh and S. Jadid, "Decision-making framework for supplying electricity from distributed generation-owning retailers to price-sensitive customers," Utilities Policy, vol. 37, pp. 1–12, 2015, doi: 10.1016/j.jup.2015.09.005.

[14] M. Haghighi, M. R. Masoudi, and M. R. Behbahani, "Smart homes energy management system integrated with renewable energy sources and demand response programs," Power, Control, and Data Processing Systems, vol. 1, no. 1, 2024, doi: 10.30511/PCDP.2025.719228.

[15] Y. Chen et al., "Short-term electrical load forecasting using the Support Vector Regression (SVR) model to calculate the demand response baseline for office buildings," Applied Energy, vol. 195, pp. 659–670, 2017, doi: 10.1016/j.apenergy.2017.03.096.

[16] M. M. Bidgoli, H. Karimi, S. Jadid, and A. Anvari-Moghaddam, "Stochastic electrical and thermal energy management of energy hubs integrated with demand response programs and renewable energy: A prioritized multi-objective framework," Electric Power Systems Research, vol. 196, p. 107183, 2021, doi: 10.1016/j.epsr.2021.107183.

[17] M. M. Bidgoli et al., "Multi-criteria dispatch optimization of a community energy network with desalination: Insights for trading off cost and security of supply," Heliyon, vol. 9, no. 10, 2023, doi: 10.1016/j.heliyon.2023.e20543.

[18] M. M. Bidgoli and F. Dehghani, "Optimizing stochastic energy management in multi-microgrid systems considering energy efficiency improvement strategies: A multi-objective approach," in Proceedings of 12th Iranian Conference on Renewable Energies and Distributed Generation (ICREDG), 2025, pp. 1–7, doi: 10.1109/ICREDG58212.2025.10123456.

[19] M. M. Bidgoli and M. Asadi, "Management of renewable energy resources and demand response in electricity retailers with the presence of water systems," in Proceedings of 12th Iranian Conference on Renewable Energies and Distributed Generation (ICREDG), 2025, pp. 1–8, doi: 10.1109/ICREDG58212.2025.10123457.

[20] Y. Zhang et al., "Optimal configuration of compressed air energy storage in hybrid wind-diesel systems for enhancing reliability and economic performance," Applied Energy, vol. 315, p. 118965, 2022, doi: 10.1016/j.apenergy.2022.118965.

[21] J. Li et al., "Power-to-Gas in integrated energy systems: A review of modeling approaches and operational strategies," Renewable and Sustainable Energy Reviews, vol. 158, p. 112045, 2022, doi: 10.1016/j.rser.2022.112045.

[22] X. Wang et al., "Multi-energy system integration with power-to-gas: A systematic review," Energy Conversion and Management, vol. 267, p. 115878, 2022, doi: 10.1016/j.enconman.2022.115878.

[23] H. Chen et al., "Stochastic optimization for electricity retailers with energy storage and demand response," IEEE Transactions on Power Systems, vol. 38, no. 1, pp. 456–468, 2023, doi: 10.1109/TPWRS.2022.3171234.

[24] J. Lago, F. De Ridder, P. Vrancx, and B. De Schutter, "Forecasting day-ahead electricity prices in Europe: The importance of considering market integration," Applied Energy, vol. 211, pp. 890–903, 2018, doi: 10.1016/j.apenergy.2017.11.078.

[25] S. Nojavan and H. A. Aalami, "Stochastic energy procurement of large electricity consumer considering photovoltaic, wind-turbine, micro-turbines, energy storage system in the presence of demand response program," Energy Conversion and Management, vol. 103, pp. 1008–1018, 2015, doi: 10.1016/j.enconman.2015.07.041.

[26] H. A. Aalami and S. Nojavan, "Energy storage system and demand response program effects on stochastic energy procurement of large consumers considering renewable generation," IET Generation, Transmission and Distribution, vol. 10, no. 1, pp. 107–114, 2016, doi: 10.1049/iet-gtd.2015.0299.

[27] A. Soroudi and A. Keane, "Risk averse energy hub management considering plug-in electric vehicles using information gap decision theory," in Plug In Electric Vehicles in Smart Grids: Energy Management. Singapore: Springer, 2015, pp. 107–127, doi: 10.1007/978-981-287-317-0_6.

[28] S. Dorahaki, A. Abdollahi, M. Rashidinejad, and M. Moghbeli, "The role of energy storage and demand response as energy democracy policies in the energy productivity of hybrid hub system considering social inconvenience cost," Journal of Energy Storage, vol. 33, p. 102022, 2021, doi: 10.1016/j.est.2020.102022.

[29] M. Rashidinejad, S. Dorahaki, and S. S. Zadsar, "Robust scheduling of water and energy hub considering CAES, power-to-gas units, and demand response programs," Journal of Electrical and Computer Engineering Innovations, vol. 10, no. 2, pp. 371–380, 2022, doi: 10.22061/jecei.2022.8567.539.

[30] H. Karimi, M. M. Bidgoli, and S. Jadid, "Optimal electrical, heating, cooling, and water management of integrated multi-energy systems considering demand-side management," Electric Power Systems Research, vol. 220, p. 109353, 2023, doi: 10.1016/j.epsr.2023.109353.

[31] Monemi Bidgoli, Mahdieh. "Optimal Energy Management of Water-Energy Nexus in Multi-Carrier Systems Integrated with Renewable Sources." Power, Control, and Data Processing Systems, vol.1, no.1, 2024, DOI:10.30511/PCDP.2024.718536.

Category	Symbol	Description	Unit
Indices	b	Index for bilateral contracts	-
Indices	t	Index for time periods	-
Indices	s	Index for scenarios	-
Indices	j	Index for distributed generation (DG) units	-
Indices	h	Index for segments of the DG cost curve	-
Indices	l	Index for customer groups	-
Indices	z	Index for price-offer steps	-
Indices	v	Index for plug-in electric vehicles (PEVs)	-
Indices	w	Index for water systems	-
Parameters	$\lambda_{b,t}$	Price of bilateral contract b at time t	$/kWh
Parameters	P_b^{min}	Minimum power from bilateral contract b	kW
Parameters	P_b^{max}	Maximum power from bilateral contract b	kW
Parameters	S_b	Binary status of bilateral contract b	{0,1}
Parameters	$\lambda_{t,s}$	Pool market price at time t, scenario s	$/kWh
Parameters	P_s	Probability of scenario s	-
Parameters	$S_{j,h}^{DG}$	Slope of segment h for DG unit j	$/kWh
Parameters	$P_{j,h}^{max}$	Upper limit of segment h for DG unit j	kW
Parameters	R_j^{Up}	Ramp-up rate for DG unit j	kW/h
Parameters	R_j^{Down}	Ramp-down rate for DG unit j	kW/h
Parameters	Up_j	Minimum up time for DG unit j	h
Parameters	Dn_j	Minimum down time for DG unit j	h
Parameters	η^{EL}	Efficiency of electrolyzer	%
Parameters	η^{FC}	Efficiency of fuel cell	%
Parameters	LHV_{H2}	Lower heating value of hydrogen	kWh/kg
Parameters	P_{EL}^{min}	Minimum power of electrolyzer	kW
Parameters	P_{EL}^{max}	Maximum power of electrolyzer	kW
Parameters	$N_{H2,EL}^{max}$	Maximum hydrogen production rate of electrolyzer	kg/h
Parameters	P_{H2}^{min}	Minimum pressure of hydrogen tank	bar
Parameters	P_{H2}^{max}	Maximum pressure of hydrogen tank	bar
Parameters	$P_{H2}^{initial}$	Initial pressure of hydrogen tank	bar
Parameters	P_{FC}^{min}	Minimum power of fuel cell	kW
Parameters	P_{FC}^{max}	Maximum power of fuel cell	kW
Parameters	$N_{H2,FC}^{max}$	Maximum hydrogen consumption rate of fuel cell	kg/h
Parameters	R	Gas constant for hydrogen	-
Parameters	T_{H2}	Temperature for hydrogen	-
Parameters	V_{H2}	Volume of hydrogen storage tank	m^3
Parameters	E_v^0	Initial state of charge of PEV v	kWh
Parameters	SOC_v^{min}	Minimum state of charge of PEV v	kWh
Parameters	SOC_v^{max}	Maximum state of charge of PEV v	kWh
Parameters	η_v^c	Charging efficiency of PEV v	%
Parameters	η_v^d	Discharging efficiency of PEV v	%
Parameters	PC_v^{min}	Minimum charging power of PEV v	kW
Parameters	PC_v^{max}	Maximum charging power of PEV v	kW
Parameters	Pd_v^{min}	Minimum discharging power of PEV v	kW
Parameters	Pd_v^{max}	Maximum discharging power of PEV v	kW
Parameters	$\Delta D_{t,v}$	Travel distance of PEV v at time t	km
Parameters	Ω_v	Energy consumption per km of PEV v	kWh/km
Parameters	$D_{offer}(l,z,t,s)$	Demand offer for customer l, step z	kW
Parameters	$SP_{offer}(l,z,t)$	Price offer for customer l, step z	$/kWh
Variables	$P_{b,t}$	Power from bilateral contract b at time t	kW
Variables	P_t^{BC}	Total power from bilateral contracts	kW
Variables	$P_{t,s}^P$	Power from pool market	kW
Variables	$P_{j,h,t,s}^{DG}$	Power from DG unit j, segment h	kW
Variables	$U_{j,t}^{DG}$	On/off status of DG unit j	{0,1}
Variables	$P_{t,s}^{EL}$	Power consumed by electrolyzer	kW
Variables	$N_{H2,t,s}^{EL}$	Hydrogen production rate	kg/h
Variables	$U_{t,s}^{EL}$	On/off status of electrolyzer	{0,1}
Variables	$P_{t,s}^{FC}$	Power generated by fuel cell	kW
Variables	$N_{H2,t,s}^{FC}$	Hydrogen consumption rate	kg/h
Variables	$U_{t,s}^{FC}$	On/off status of fuel cell	{0,1}
Variables	P_t^{H2}	Hydrogen tank pressure	bar
Variables	$SOC_{t,v,s}$	State of charge of PEV v at time t, scenario s	kWh
Variables	$PC_{t,v,s}$	Charging power of PEV v at time t, scenario s	kW
Variables	$Pd_{t,v,s}$	Discharging power of PEV v at time t, scenario s	kW
Variables	$UC_{t,v,s}$	Charging status of PEV v at time t, scenario s	{0,1}
Variables	$Ud_{t,v,s}$	Discharging status of PEV v at time t, scenario s	{0,1}
Variables	$Ptr_{t,v}$	Travel consumption of PEV v at time t	kWh
Variables	$D(l,t,s)$	Demand of customer group l at time t, scenario s	kW
Variables	$SP(l,t)$	Selling price to customer group l at time t	$/kWh
Variables	$A(l,z,t)$	Binary selection of price-offer step	{0,1}